energies

MDPI

Article

Method of Improving Lateral Stability by Using Additional Yaw Moment of Semi-Trailer

Zhenyuan Bai, Yufeng Lu * and Yunxia Li

School of Mechanical and Automotive Engineering, Qilu University of Technology (Shandong Academy of Sciences), Jinan 205353, China; bzy884406179@126.com (Z.B.); ldyffr@126.com (Y.L.)

* Correspondence: luyf@qlu.edu.cn

Received: 20 October 2020; Accepted: 26 November 2020; Published: 30 November 2020

Abstract: The lateral stability control of tractor semi-trailer plays a vital role for enhancing its driving safety, and the distributed electric drive structure of a hub motor creates opportunities and challenges for realising the lateral stability accurately. Based on the dynamics simulation software TruckSim, a nonlinear dynamic tractor semi-trailer model is established, and a MATLAB/Simulink linear three-degree-of-freedom monorail reference model is established. The upper controller adopts fuzzy proportional–integral–derivative control to export active yaw torque values of the tractor and semi-trailer. The lower controller outputs the driving/braking torque of each wheel according to the target wheel driving/braking rules and torque distribution rules. The tractor produce an active yaw torque through conventional differential braking the hub motor is installed on both sides of the semi-trailer, and the active yaw torque is produced by the coordinated control of the driving/braking torque of the hub motor and the differential braking of the mechanical braking system. To prevent wheel locking, the slip rate of each wheel is controlled. Finally, based on the TruckSim–MATLAB/Simulink cosimulation platform, cosimulation is performed under typical working conditions. The simulation results show that the control strategy proposed in this report is superior to the conventional differential braking control (ESP). It can not only improve the lateral stability of the vehicle more effectively, but also improve the roll stability.

Keywords: tractor semi-trailer; lateral stability; hub motor; differential braking; coordination

1. Introduction

In recent years, tractor semi-trailers have become a major means in the field of transportation due to their economical and efficient advantages [1]. However, because of its characteristics of a long body, complex structure, high centroid at full load, and rear amplification, the tractor semi-trailer is prone to lose lateral stability, for example sideslip; drift; and jackknife, when driving on low adhesion coefficient roads, such as roads affected by rain, snow, and wetness. Since a fully loaded trailer is much heavier than a tractor, the trailer plays a vital role in the lateral stability control of the entire vehicle [2–4]. According to the 2016 statistical report of the Federal Automobile Transportation Administration of the United States Department of Transportation, heavy truck traffic accident deaths accounted for 10% of all traffic accident deaths, and tractor semi-trailers accounted for 61% [5]. The lateral instability of tractor semi-trailers is the main factor in traffic accidents [6]. Increasing environmental pollution and energy depletion have accelerated the research progress of distributed electric vehicles [7–10]. The rear wheel hub drive vehicle is driven by distributed power. Through the accurate control of the wheel hub motor of the rear wheel hub drive vehicle, the handling and safety of the vehicle can be significantly improved [11–13]. Many scholars have researched the lateral stability control of tractor semi-trailers and hub-driven vehicles.

Seyed Hossein et al. [14] proposed an adaptive control algorithm that combined yaw moment with differential braking based on the Lyapunov direct method. The algorithm was used to estimate unknown parameters of the vehicle, and the final results showed that the adaptive control algorithm can improved the vehicle driving stability effectively. Takenaga et al. [15] proposed a tractor semi-trailer path tracking controller based on the fuzzy control law and built a joint controller of travel path error feedback and driver preview feedforward, effectively ensuring the tracking of the ideal path for the tractor semi-trailer. Kharrazi [16] proposed a robust control policy to improve the yaw stability performance of a heavy multi-trailer considering the variation of parameters, and the control results showed that the control strategy greatly reduced the magnification of the rear end, and the braking system did not interfere with the steering system of the tractor. Yang et al. [17] built a vehicle lateral stability controller based on MATLAB/Simulink. The upper controller and the lower controller are, respectively, responsible for the production of active torque and the distribution of braking torque; the strategy improved the yaw stability and roll stability of the entire vehicle. Eunhyek et al. [18] designed an integrated chassis control strategy for four-wheel braking and front/rear axle drive torque with the goal of improving the tire slip ratio and implemented the optimal allocation of braking and driving moments using a monitor-based hierarchical structure. Chen et al. [19] proposed two different control methods for the stability control of wheel drive electric vehicles, namely, unsteady state control and continuous control, and adopted sliding mode controller to control the stability of the vehicle in unstable state. Chae et al. [20] used the multi-modal sliding mode controller to improve the driving stability of hub-driven electric vehicles and solved the problem of controller robustness under the condition of variable parameters. Huang et al. [21] developed a transverse stability control strategy for vehicles driven by hub motors based on regional pole assignment. The combined action of the driving force of hub motors and the braking force that generates the additional yawing torque is utilized; the simulation results showed that this strategy can improve the vehicle handling stability and achieve torque distribution more reliably. Wang Zhenbo et al. [22] developed the stability control strategy of four-wheel independent drive electric vehicle (FWIA-EV) based on optimal control to improve the vehicle handling stability. This control strategy performs better than the rule-based control strategy and has the ability of online implementation. Changfu Zong et al. [23] used the method of independently defining the understeer gradient of the tractor and the semitrailer to study the handling stability of the semitrailer train and analyzed the impact of vehicle structural parameters on the understeer grads. Xiujian Yang et al. [24] investigated a strategy to independently control the direct yawing torque of the tractor and trailer in order to study the stability of the lower semi-trailer under extreme operation, which reduced the complexity of the brake wheel selection decision and obtain a better control effect.

At present, most research on the lateral stability of tractor semi-trailers is based on improving the performance of a single aspect of the vehicle, such as braking, driving, steering, or suspension, which have some deficiencies. Differential braking control is a mature and overall tactics to enhance vehicle driving stability [25]. The wheel hub motor is independent and controllable, with high transmission efficiency and accurate and rapid torque output. In comparison with traditional vehicles, it has unique advantages in stability control. When the regenerative braking condition is met, some of the vehicle's kinetic energy will be transformed into electric energy for recycling. This can not only improve the energy utilization rate, but also reduce the wear of the mechanical braking system [26–30]. However, at present, the research on improving the lateral stability of vehicles through a hub motor is mainly for passenger cars, and there is little research on tractor semi-trailers. Giving the shortcomings of the existing research, we proposed a coordinated control strategy in the area of hub motor and differential braking. By installing hub motors on both sides of the semi-trailer, taking advantage of its distributed drive structure, the lateral stability of the tractor semi-trailer is improved.

2. Dynamic Model

2.1. Nonlinear Tractor Semi-Trailer Model

A nonlinear tractor semi-trailer model was established by using the vehicle dynamics simulation software TruckSim, in which 2A Tractor w/1A Van Trailer was selected as the real vehicle model, including a tractor steering shaft, a driving shaft, and semi-trailer axle. Modelling for the overall appearance was carried out, as shown in Figure 1. The main parameters of the TruckSim model are revealed in Table 1 [31].

Figure 1. Establishment of TruckSim nonlinear vehicle model.

Table 1. Main parameters of TruckSim model [31].

Category	Value		Unit
	Tractor	Semi-Trailer	
No-load mass	4457	6000	kg
Yaw inertia	34,823	54,000	Kg m^2
Roll inertia	2287	10,140	Kg m^2
Wheelbase	3500	6700 (to hinge point)	m
Wheel distance	2030/1863	1863	mm
Wheel radius	510/510	510	mm
Centroid height	1173	1935	mm
Maximum brake pressure	0.7	0.7	mpa
Engine power	225	-	kw
Transmission	7-speed MT	-	-

2.2. Reference Model

In this paper, the reference model adopts a simplified four degrees of freedom monorail yaw model, which can produce the require yaw rate of tractor semi-trailer, as shown in Figure 2. The standard expression form of the model is shown in Equations (1)–(4).

$$m_1 a_{y1} = F_{y1} + F_{y2} - F_{hy} \tag{1}$$

$$I_{z1}\dot{\gamma}_1 = F_{y1}a_1 - F_{y2}b_1 + F_{hy}l_p \tag{2}$$

$$m_2 a_{y2} = F_{y3} + F_{hy} \tag{3}$$

$$I_{z2}\dot{\gamma}_2 = F_{hy}a_2 - F_{y3}b_2 \tag{4}$$

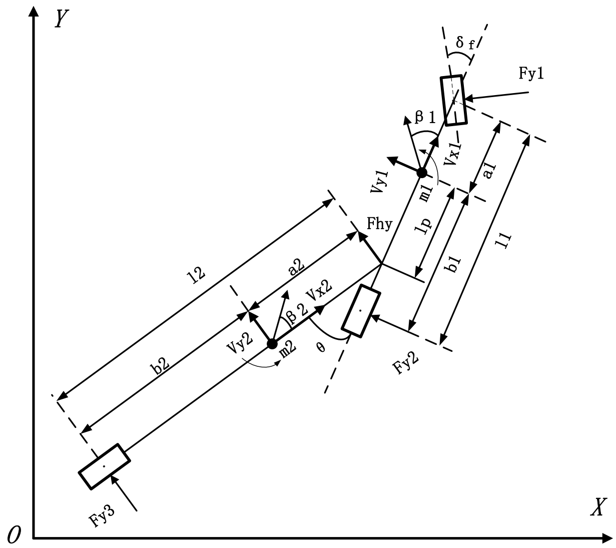

Figure 2. Linear four degrees of freedom monorail reference model.

In the formula, m_1 and m_2 are the mass of the tractor and semi-trailer, respectively; I_{z1} and I_{z2} are the yaw moment of inertia of the tractor and semi-trailer, respectively; γ_1 and γ_2 are the yaw rate of the tractor and semi-trailer, respectively; F_{y1}, F_{y2}, and F_{y3} correspond to the lateral tire forces of the front axle of the tractor, the rear axle of the tractor, and the semi-trailer tires; F_{hy} is the lateral pulling force between the tractor and the semi-trailer; a_1 and b_1 are the distances from tractor centroid to its front and rear axles; a_2 and b_2 are the distances from trailer centroid to towing point and trailer axle; l_p is the distance from tractor centroid to towing point; a_{y1} and a_{y2} are the lateral acceleration of the tractor and semi-trailer, respectively, and

$$a_{y1} = \dot{v}_{y1} + v_{x1}\gamma_1$$

$$a_{y2} = \dot{v}_{y1} + v_{x1}\gamma_1 - l_p\dot{\gamma}_1 - a_2\left(\dot{\gamma}_1 + \ddot{\theta}\right) + v_{x1}\dot{\theta}$$

In the following, approximate assumptions $v_{x1} = v_{x2} = v_x$. Here, v_{x1} is the longitudinal speed of tractor, v_{x2} is the longitudinal speed of trailer.

The yaw rate conforms to the following formula:

$$\gamma_2 = \gamma_1 + \dot{\theta} \tag{5}$$

The lateral force of the axletrees of the tractor semi-trailer can be approximated as the following formula:

$$F_{yi} = K_{yi}\alpha_i \tag{6}$$

In the formula, i takes 1, 2, 3; K_{y1}, K_{y2}, K_{y3}, respectively, represent the cornering characteristics of the tractor's front and rear axletree wheels and the trailer's tires; α_1, α_2, α_3, respectively, represent the sideslip angles of the tractor's front and rear axle wheels and the trailer's wheels, and

$$\alpha_1 = \delta_f - \frac{\left(v_{y1} + \alpha_1\gamma_1\right)}{v_x} \tag{7}$$

$$\alpha_2 = \frac{\left(b_1\gamma_1 - v_{y1}\right)}{v_x} \tag{8}$$

$$\alpha_3 = \theta - \frac{\left(v_{y1} - \left(l_p + l_2\right)\gamma_1 - l_2\dot{\theta}\right)}{v_x} \tag{9}$$

From Equations (1)–(9), the steady-state response expression of the tractor's yaw rate of the tractor semi-trailer can be obtained as:

$$\gamma_1{}^* = \frac{v_x}{l_1\left(1+K_s v_x^2\right)}\delta_f \tag{10}$$

among them,

$$K_s = \frac{b_1 l_2 m_1 + \left(b_1 - l_p\right) b_2 m_2}{l_1^2 l_2 K_{y1}} - \frac{a_1 l_2 m_1 + \left(a_1 + l_p\right) b_2 m_2}{l_1^2 l_2 K_{y2}} \tag{11}$$

It can be obtained from Equation (5) that the yaw rate of the semi-trailer and the tractor is equal when turning in a steady state, that is, $\gamma_2{}^* = \gamma_1{}^*$

2.3. Hub Motor Model

The hub motor produces active yaw torque by applying requirement torque to the tire to enhance the trailer's lateral stability. We choose the permanent magnet synchronous motor as the hub motor because of its high power density, high power, and small torque ripple. The idea expression is

$$T_m = \frac{1}{\tau s+1} T_e \tag{12}$$

where T_m is the motor output torque, T_e is the expected torque of the motor, and s is the Laplace transform operator.

It is assumed that the motor control system can achieve the desired torque accurately, but the phase difference interval is τ; in addition, the motor's output torque is restricted by the maximum torque.

$$-T_{max} \le T_m \le T_{max} \tag{13}$$

3. Design of Control System

3.1. The General Architecture of the Control System

The reference model takes the front wheel angle output by TruckSim as the input, outputs the ideal value of yaw rate of the tractor and semi-trailer, and the yaw rate deviations e_1 and e_2 are obtained, respectively, after determining the difference from the actual yaw rate output of TruckSim. The upper controller takes the e and ec as input, and outputs the additional tractor and semi-trailer yaw moments ΔM_1 and ΔM_2, respectively. The lower controller allots the driving torque and braking torque generated by the wheel hub motor and the mechanical braking torque of the semi-trailer. Finally, to prevent wheel locking, the slip rate of each wheel is monitored by the slip rate controller. The control logic structure is illustrated in Figure 3.

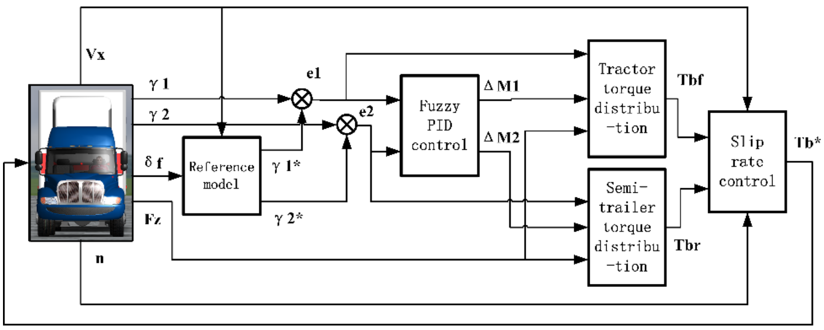

Figure 3. Control flowchart of lateral stability of tractor semi-trailer.

3.2. Upper Controller

The control of the tractor semi-trailer needs to be real time and complex; compared with single proportional–integral–derivative (PID) control and fuzzy control, the fuzzy proportional–integral–derivative (PID) control can not only introduce people's control experience and methods and standardize, but also realize the automatic adjustment of parameters K_p, K_i, and K_d to meet the control of nonlinear system [32], so the upper controller adopts fuzzy PID control. The upper controller takes the deviation e and variation rate ec of the actual yaw rate and reference yaw rate of the tractor and trailer as the input, and the additional yaw moment ΔM_1 and ΔM_2 of the tractor and trailer as the output. The fuzzy PID control adaptive structure is depicted in Figure 4 [33,34].

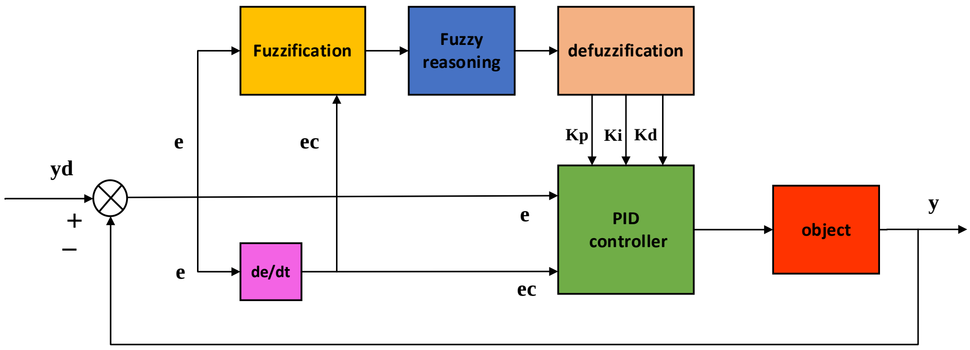

Figure 4. Fuzzy proportional–integral–derivative (PID) control structure [33,34].

The fuzzy universe of *e* and *ec* is [−3, 3], which obeys a Gaussian distribution. The fuzzy universe of the outputs K_p, K_i, and K_d is [0, 1], which obeys a trigonometric function. The fuzzy input and output language variables are ml (minus large), mm (minus middle), ms (minus small), ze (zero), ps (plus small), pm (plus middle), and pl (plus large)—seven fuzzy language sets. The membership functions of e, ec, K_p , K_i, and K_d are shown in Figure 5. The surface relationship between input parameters and output parameters of fuzzy PID control is shown in Figure 6. The fuzzy rules of outputs K_p, K_i, and K_d are presented in Tables 2–4 [33,35].

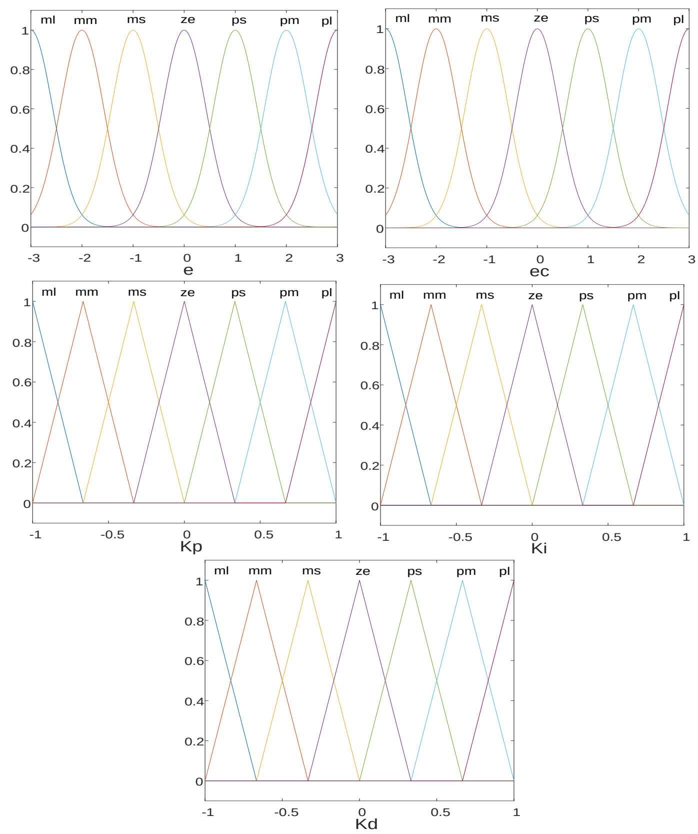

Figure 5. Membership functions of e, ec, K_p, K_i, and K_d [33,34].

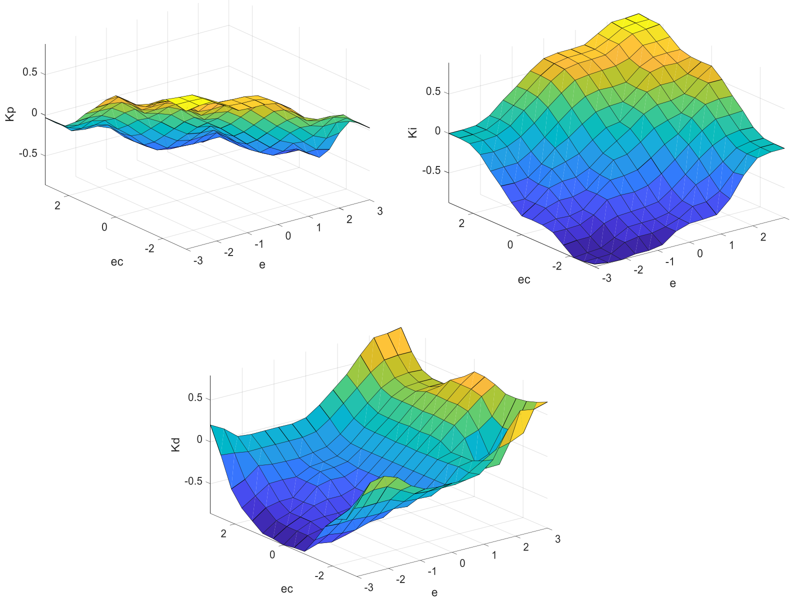

Figure 6. Surface relationship between input and output.

Table 2. Fuzzy rule table of K_p.

K_p		ec						
		ml	**mm**	**ms**	**ze**	**ps**	**pm**	**pl**
	ml	pl	pl	pl	pm	ps	ze	ze
	mm	pl	pl	pm	ps	ps	ze	ms
	ms	pm	pl	ps	ps	ze	ms	ms
e	ze	pm	pm	ps	ze	ms	mm	mm
	ps	ps	ps	ze	ms	ms	mm	mm
	pm	ps	ze	ms	mm	mm	mm	ml
	pl	ps	ze	mm	mm	mm	ml	ml

Table 3. Fuzzy rule table of K_i.

K_i		ec						
		ml	**mm**	**ms**	**ze**	**ps**	**pm**	**pl**
	ml	pl	pl	pl	pm	ps	ze	ze
	mm	pl	pl	pm	ps	ps	ze	ms
	ms	pm	pl	ps	ps	ze	ms	ms
e	ze	pm	pm	ps	ze	ms	mm	mm
	ps	ps	ps	ze	ms	ms	mm	mm
	pm	ps	ze	ms	mm	mm	mm	ml
	pl	ps	ze	mm	mm	mm	ml	ml

Table 4. Fuzzy rule table of K_d.

K_d		ec						
		ml	**mm**	**ms**	**ze**	**ps**	**pm**	**pl**
	ml	ms	ms	ml	ml	ml	mm	ps
	mm	ps	ms	ml	mm	mm	ms	ze
	ms	ze	ms	mm	mm	ms	ms	ze
e	ze	ze	ms	ms	ms	ms	ms	ze
	ps	ze	ze	ze	ze	ze	ze	ps
	pm	pl	ms	ps	ps	ps	ps	pl
	pl	pl	pm	pm	pm	ps	ps	pl

3.3. Lower Controller

General brake torque distribution rules have some shortcomings: single-wheel braking may cause a larger braking torque to concentrate on one wheel, easily resulting in locking. Single-side braking efficiency is low. Full braking makes the semi-trailer unable to produce additional yaw moment, which easily causes sideslip, jackknifing, and other unstable phenomena. The lower-level torque distribution strategy proposed determines the target drive/brake wheels and distributes the drive/brake torque according to the additional yaw moment, steering direction, yaw rate deviation, wheel vertical load, and other signals output by the upper-level controller.

3.3.1. Determination of Braking Torque

1. Moment allocation of tractor

The active yaw torque ΔM_1 of the tractor is produced by differential braking. The relation between the active yaw torque and the braking torque of tractor semi-trailer is indicated in Figure 7.

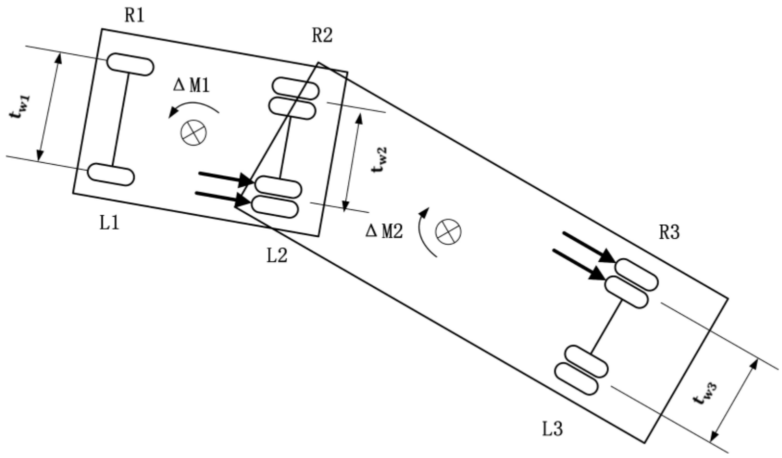

Figure 7. Relationship between yaw torque and braking force of tractor semi-trailer.

The two tires with adjacent coaxial lines are simplified to a single tire. Assuming that the braking moment of the wheel when the wheel is not locked is approximately proportional to its vertical load; the braking moment of every tire of the tractor is shown below.

(i) When $\Delta M_1 > 0$, it is necessary to brake the left wheel, and the braking moments of each wheel on the left side of the tractor are as follows:

$$T_{L1} = F_{XL1}R_1 = \frac{F_{ZL1}}{F_{ZL1}+F_{ZL2}} \cdot \frac{4\Delta M_1}{t_{w1}+t_{w2}} \cdot R_1 \tag{14}$$

$$T_{L2} = F_{XL2}R_2 = \frac{F_{ZL2}}{F_{ZL1}+F_{ZL2}} \cdot \frac{4\Delta M_1}{t_{w1}+t_{w2}} \cdot R_2 \tag{15}$$

where F_{XL1} and F_{XL2} are the longitudinal braking force of the left wheels on the front and rear axle of the tractor, respectively; F_{ZL1} and F_{ZL2} are the vertical loads on the left wheel of the front and rear axis of the tractor, respectively; t_{w1} and t_{w2} are the track widths of the front and rear axles of the tractor, respectively; and R_1 and R_2 are the rolling radius of the front and rear axle wheels of the tractor, respectively.

(ii) When $\Delta M_1 < 0$, it is necessary to brake the right wheel, and the braking moments of each wheel on the right side of the tractor are as follows:

$$T_{R1} = F_{XR1}R_1 = \frac{F_{ZR1}}{F_{ZR1}+F_{ZR2}} \cdot \frac{4\Delta M_1}{t_{w1}+t_{w2}} \cdot R_1 \tag{16}$$

$$T_{R2} = F_{XR2}R_2 = \frac{F_{ZR2}}{F_{ZR1}+F_{ZR2}} \cdot \frac{4\Delta M_1}{t_{w1}+t_{w2}} \cdot R_2 \tag{17}$$

where F_{XR1} and F_{XR2} are the longitudinal braking force of the right wheels on the front and rear axis of the tractor, respectively, and F_{ZR1} and F_{ZR2} are the vertical loads on the right wheel of the front and rear axle of the tractor, respectively.

2. Moment Allocation of semi-trailer

The tire on both sides of the semi-trailer are equipped with hub motors. First, the torque distribution control method combining differential drive and differential braking used as realize part of additional yaw torque—that is, the differential drive of one wheel hub motor and the differential braking of the other wheel hub motor are adopted. In comparison with the differential braking or differential drive alone, the adhesion requirements of the road surface are significantly reduced, the torque output of the wheel is reduced, and the adhesion between the tire and the ground is improved. The principle display as Figure 8.

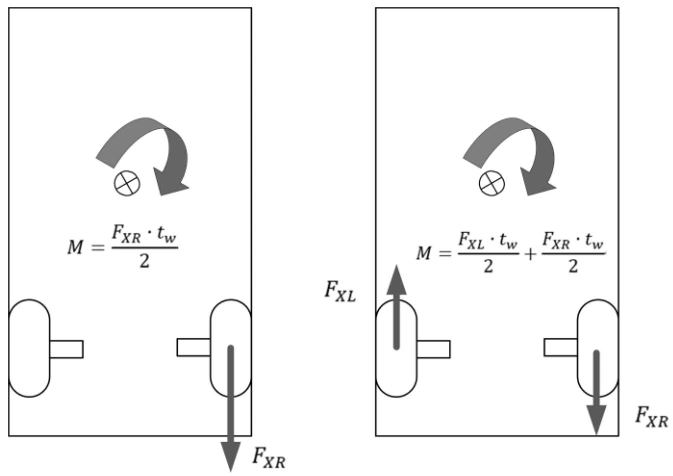

Figure 8. Principle of yaw moment produced by braking force and driving force at the same time.

Because of the small braking (driving) capacity of the motor in the power system of the wheel hub motor, the ability to generate yaw moment is limited, so mechanical braking is adopted for the part that does not meet the requirements. The collaborative control strategy is shown in Figure 9. At the same time, the design capacity of the brake can be reduced because of the electric braking capacity of the wheel motor.

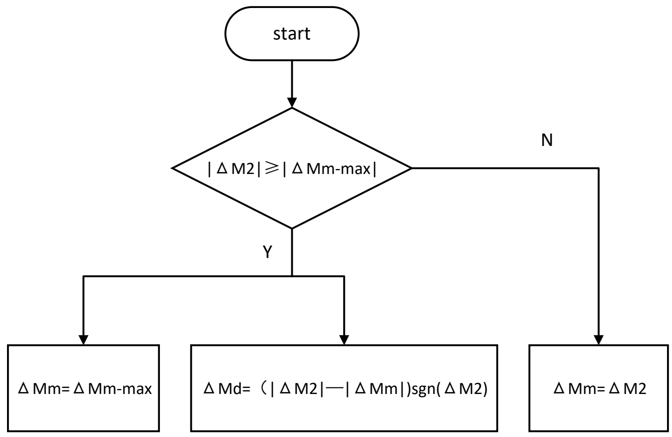

Figure 9. Cooperative control strategy chart.

Here, ΔM_{m-max} is the maximum yaw moment provided by output torque of hub motors on both sides of semi-trailer, ΔM_m is the active yaw torque to be produced by the hub motor, and ΔM_d is the active yaw torque to be produced by the semi-trailer mechanical braking system.

The maximum yaw torque to the semi-trailer centroid when driven by a single wheel hub motor is as follows:

$$\Delta\hat{M}_m = \frac{\Delta M_{m-max}}{2} = \frac{T_{max}t_{w3}}{2R_3} \tag{18}$$

where T_{max} is the largest output torque of the hub motor, t_{w3} is the wheel track of the semi-trailer, and R_3 is the wheel rolling radius of the semi-trailer.

Taking $\Delta M_2 > 0$ as an example, the torque distribution strategy is further explained. It stipulates that the braking moment is positive and the driving moment is negative. At this time, L3 is braking and R3 is driving (when $\Delta M_2 < 0$, it is only necessary to change the left and right rounds in the strategy and consider the absolute value of ΔM_2 for the calculation).

(i) When $\Delta\hat{M}_m \geq 0.5\Delta M_2$, the yaw moment a of the semi-trailer ΔM_2 is provided by the wheel hub motor, and the torque distributed by the wheel of the semi-trailer is as follows:

$$T_{L3} = -T_{R3} = \frac{\Delta M_2 * R_3}{t_{w3}} \tag{19}$$

(ii) When $\Delta\hat{M}_m < 0.5\Delta M_2$, the active yaw torque is first provided by the hub motor, and the insufficient additional yaw moment is provided by mechanical braking. The moment allocated by the wheels of the semi-trailer are as follows:

$$T_{R3} = -T_{max} \tag{20}$$

$$T_{L3} = T_{max} + T_d = \frac{2R_3\Delta M_2 - 2\Delta\hat{M}_m}{t_{w3}} \tag{21}$$

Here, T_d is the mechanical braking torque of the semi-trailer wheel.

3.3.2. Formulation of Target Wheel Braking (Driving) Rules

The curve of the relationship between the additional yaw torque and the portrait ground braking force of every tire is indicated in Figure 10. The Figure 10 indicates that applying the braking torque to the outer front wheel and outer rear wheel leads to understeering; the outer front wheel has a higher efficiency. In contrast, applying the braking torque to the inner front wheel and inner rear wheel leads to excessive steering; the inner rear wheel has a higher efficiency [36]. It is ruled that the front wheel turns left in a positive direction, and the yaw velocity and active yaw torque are positive in the counterclockwise direction. The decision rules for the target wheel of the tractor are presented in Table 5, and those for the semi-trailer are presented in Table 6.

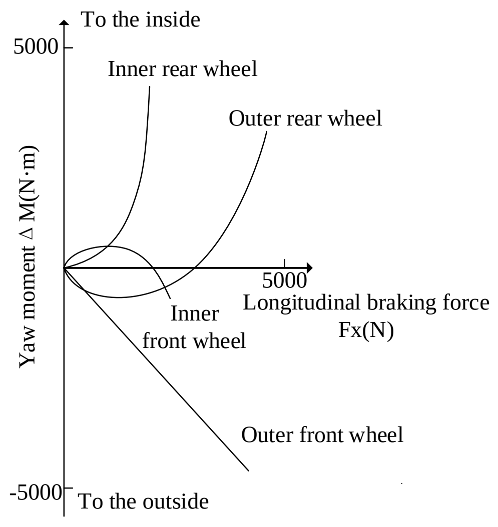

Figure 10. Variation curve of vehicle yaw moment and wheel longitudinal braking force.

Table 5. Decision rules for target wheel of tractor.

Reference Yaw Rate (γ_1^*)	Actual Yaw Rate (γ_1)	Yaw Rate Deviation ($e_1 = \gamma_1^* - \gamma_1$)	Steering Characteristics	Target Brake Wheel
+	+	+	understeer	L2
+	+	−	oversteer	R1
+	+	0	neutral steer	\
+	0	+	understeer	L2
+	−	+	understeer	L1
0	−	+	oversteer	L1
0	+	−	oversteer	R1
0	0	0	neutral steer	\
−	−	−	understeer	R2
−	−	+	oversteer	L1
−	−	0	neutral steer	\
−	+	−	understeer	R1
−	0	−	understeer	R2

Table 6. Decision rules for target wheel of semi-trailer.

Reference Yaw Rate (γ_2^*)	Actual Yaw Rate (γ_2)	Yaw Rate Deviation ($e_2 = \gamma_2^* - \gamma_2$)	Steering Characteristics	Target Wheel	
				Drive	Brake
+	+	+	understeer	R3	L3
+	+	−	oversteer	L3	R3
+	+	0	neutral steer	\	\
+	0	+	understeer	R3	L3
+	-	+	understeer	R3	L3
0	-	+	oversteer	R3	L3
0	+	−	oversteer	L3	R3
0	0	0	neutral steer	\	\
−	−	−	understeer	L3	R3
−	−	+	oversteer	R3	L3
−	−	0	neutral steer	\	\
−	+	−	understeer	L3	R3
−	0	−	understeer	L3	R3

4. Slip Rate Controller

After determining the driving (braking) torque distribution of the target wheel, to ensure that the wheel does not lock and further improve the lateral stability, slip rate control is applied to each wheel. The real-time slip rate can be obtained by the speed u and wheel speed n output by TruckSim. The slip ratio calculation formula is as follows:

$$\lambda = \frac{u - r\omega}{u} \tag{22}$$

where u is the vehicle linear velocity, r is the tire radius, and ω is the wheel angular speed.

Guo et al. [37] pointed out that the variation range of the tire slip rate λ corresponding to the maximum longitudinal adhesion coefficient φ_{Lmax} is generally between 0.08 and 0.3. The curves of the tire longitudinal and lateral adhesion coefficient versus slip rate are depicted in Figure 11.

Considering the safety of the vehicle in extreme conditions, the wheel slip ratio of the tire is controlled between 0.15 and 0.20. The values of the increase rate K_i and decline rate K_d are

$$\begin{cases} K_i = \frac{5000Nm}{s} \\ K_d = \frac{5000Nm}{s} \end{cases}. \tag{23}$$

The output value T_D of the adjusted braking torque is

$$\begin{cases} T_{(t+1)} = T_{(t)} + K_i T_s,\ S < 0.15 \\ T_{(t+1)} = T_{(t)},\ 0.15 < S < 0.20 \\ T_{(t+1)} = T_{(t)} - K_d T_s,\ S > 0.20 \end{cases} \tag{24}$$

where $T_{(t)}$ is the output value of the braking torque at moment t, $T_{(t+1)}$ is the output value of the braking torque at moment $t+1$, and T_s is the calculation step size.

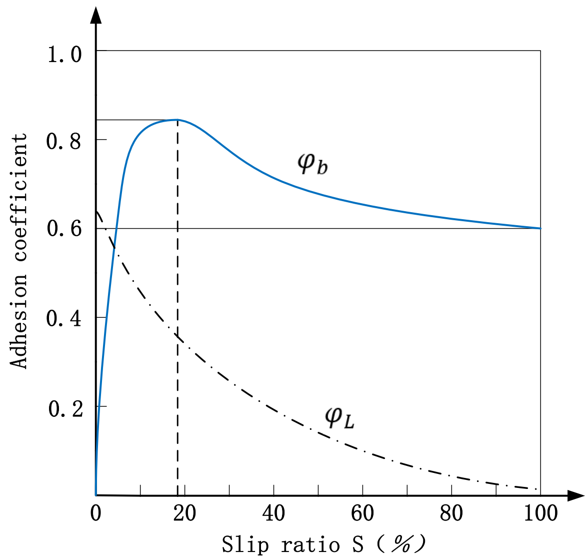

Figure 11. Relation of tire longitudinal and lateral adhesion coefficient versus slip rate.

5. Simulation Analysis

A nonlinear vehicle model was built in TruckSim, and its S-function was output to MATLAB/ Simulink. Double lane change and steering wheel angle step were selected as the input conditions for the joint simulation of TruckSim and Simulink

5.1. Double-Lane-Change Condition

The initial velocity was defined as v_{x1} = 100 km/h, and the road surface adhesion coefficient was set to 0.3. From the comparison of animation simulation in Figure 12, it can be seen that without control, the semi-trailer has obvious sideslip, has deviated from the track, the tractor has a large roll, and the whole vehicle loses the ability to track the path; after the cooperative and differential controls are added, the tractor semi-trailer completed the double-lane-change test, and the roll amplitude was also significantly improved. The steering wheel angle input curve is shown in Figure 13. The yaw rate of the semi-trailer and the maximum sideslip angle of the semi-trailer are important indices for evaluating the yaw stability of the tractor semi-trailer. Figures 14 and 15 show that, without control, the yaw rate of the tractor increases continuously after 8 s and reaches the peak value of 45°/s at 12 s; the yaw rate of the semi-trailer reaches a peak value of 73.68°/s at 8 s, and the tractor semi-trailer has serious sideslip. After the cooperative and differential controls are added, the absolute value of the peak yaw rate of the tractor decreases to 28.68 and 30.19°/s, respectively, and the absolute value of the peak yaw rate of the semi-trailer decreases to 48.54 and 40.43°/s, respectively. At 10.5 s, the yaw rate of the tractor and semi-trailer converges to 0 and is finally stable. Figures 16 and 17 show that, after adding the cooperative and differential controls, the absolute value of the centroid sideslip angle of the tractor decreases from 92.83° before the control to 8.67 and 10.92°, respectively, and the absolute value of the semi-trailer centroid sideslip angle decreases from 61.02° before the control to 25.66 and 39.79°, respectively. In comparison with the differential braking control, the coordinated control makes the centroid sideslip angle of the tractor and semi-trailer converge to 0 faster. The hinge angle is the main index to characterize the jackknife stability of the tractor semi-trailer. Figure 18 shows that, after coordinated control and differential braking control are added, the absolute value of the articulation angle decreases from 93.32° (folding instability occurred) before control to 27.11 and 44.76°, respectively. In comparison with differential braking control, collaborative control can make the hinge angle converge to 0 faster. Figures 19 and 20 show that, without control, the roll angle of the tractor reaches the peak value of 4.17° at 7 s, the roll angle of the semi-trailer fluctuates greatly, and reaches the peak value of 6.81° at 13 s; after the cooperative and differential controls are added, the roll angle of the peak roll angle of the tractor decreases to 2.01 and 2.29°, respectively, and the peak roll angle of the semi-trailer decreases to 2.96 and 2.51°, respectively. At 11s, the roll angle of the tractor semi-trailer converges to 0 and is finally stable. Figures 21 and 22 show that, after adding the cooperative and differential controls, the absolute value of the lateral acceleration of the tractor decreases from 8.14° before the control to 7.27 and 7.35°, respectively, and the absolute value of the semi-trailer centroid sideslip angle decreases from 7.06° before the control to 4.60 and 5.21°, respectively.

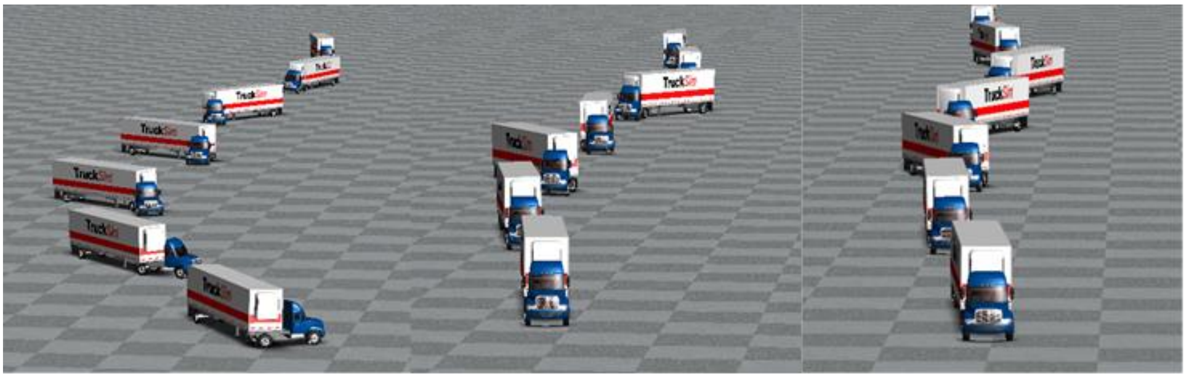

(a) With control (b) Differential braking control (c) coordinated control

Figure 12. Simulation animation comparison.

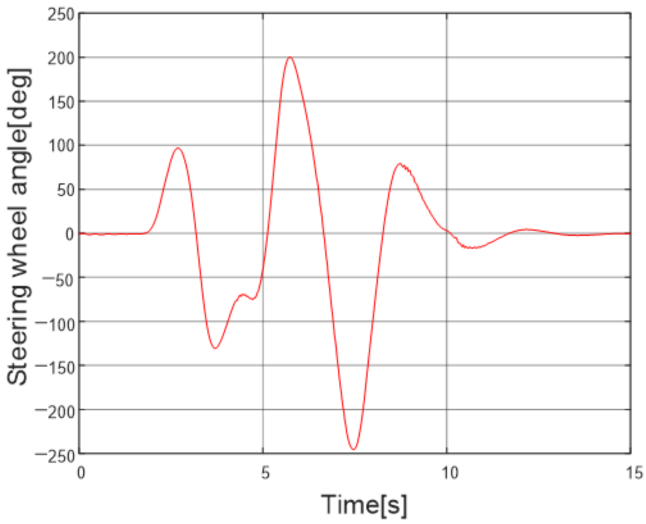

Figure 13. Steering wheel.

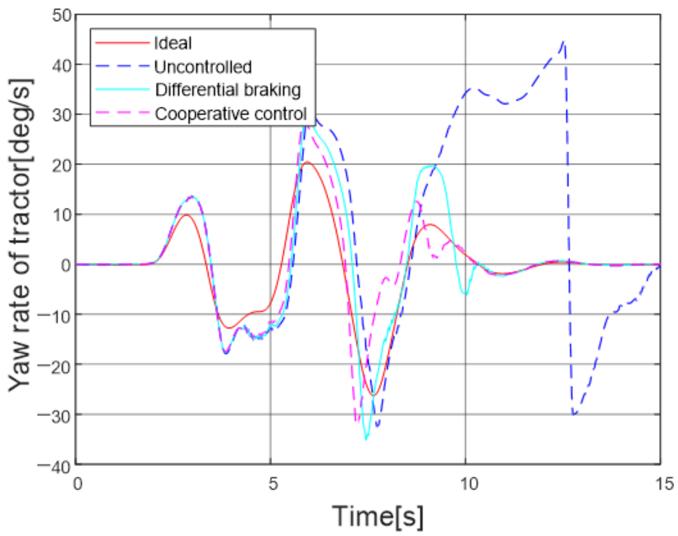

Figure 14. Yaw rate of tractor.

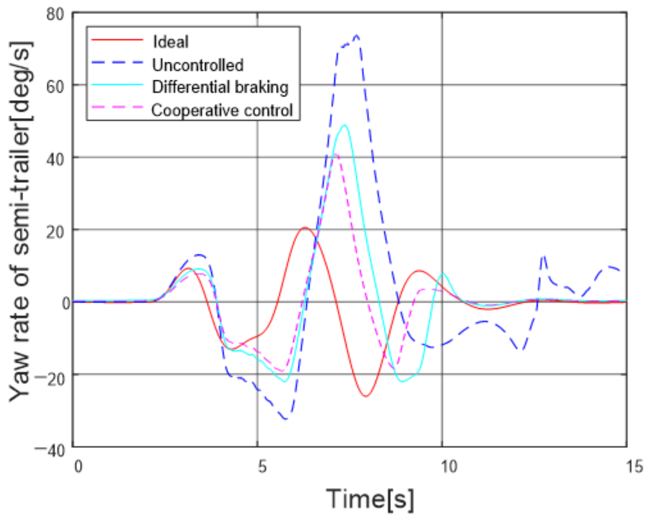

Figure 15. Yaw rate of semi-trailer.

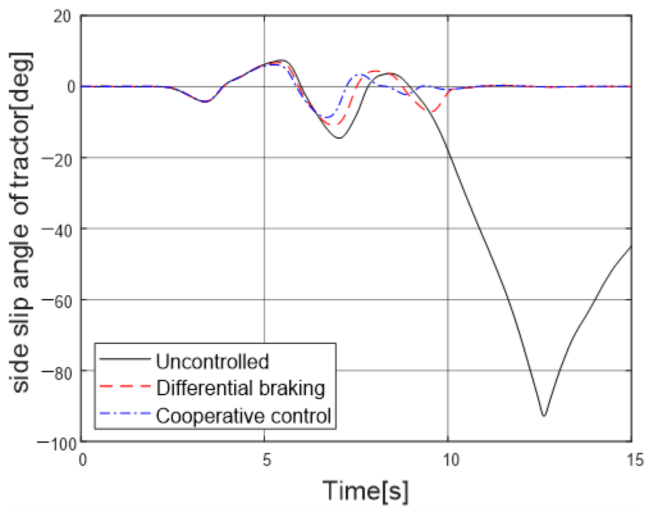

Figure 16. Sideslip angle of tractor.

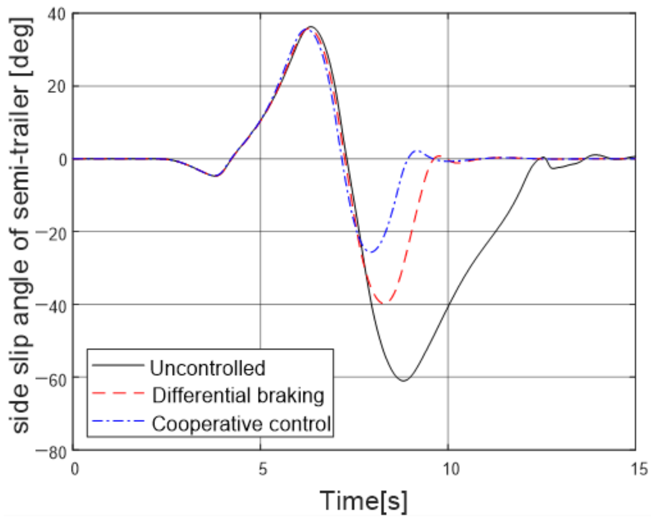

Figure 17. Sideslip angle of semi-trailer.

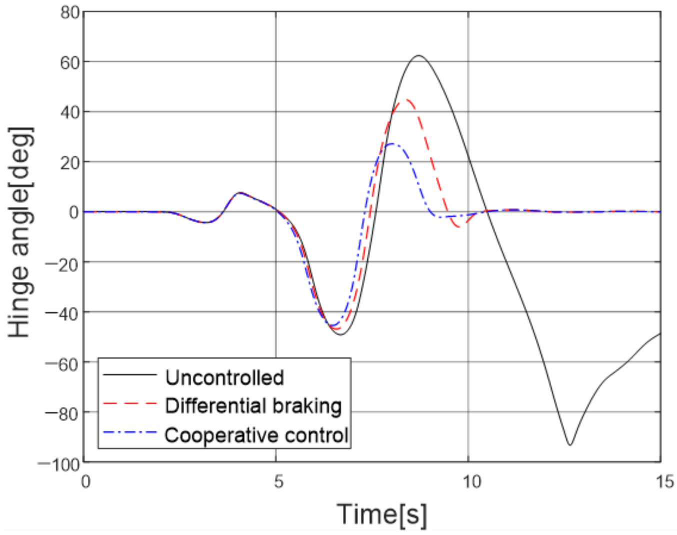

Figure 18. Hinge angle.

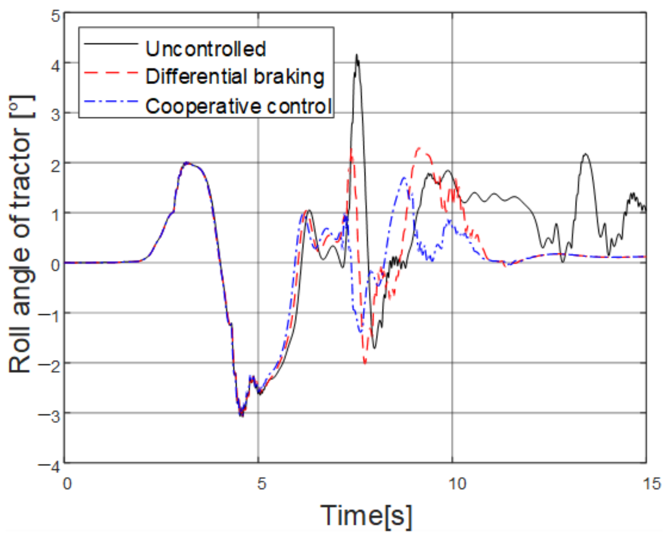

Figure 19. Roll angle of tractor.

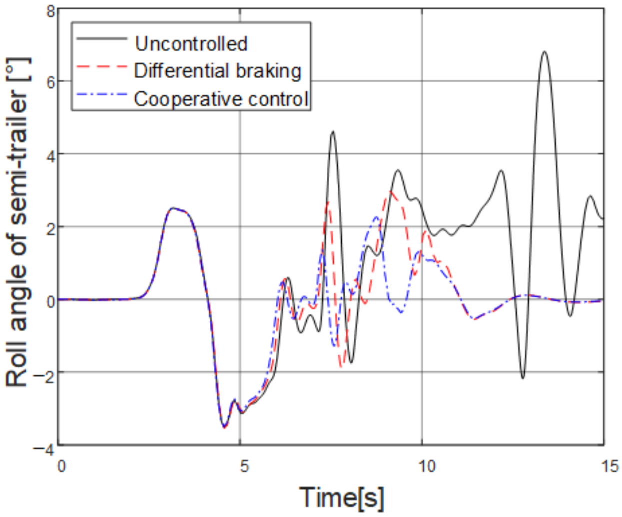

Figure 20. Roll angle of semi-trailer.

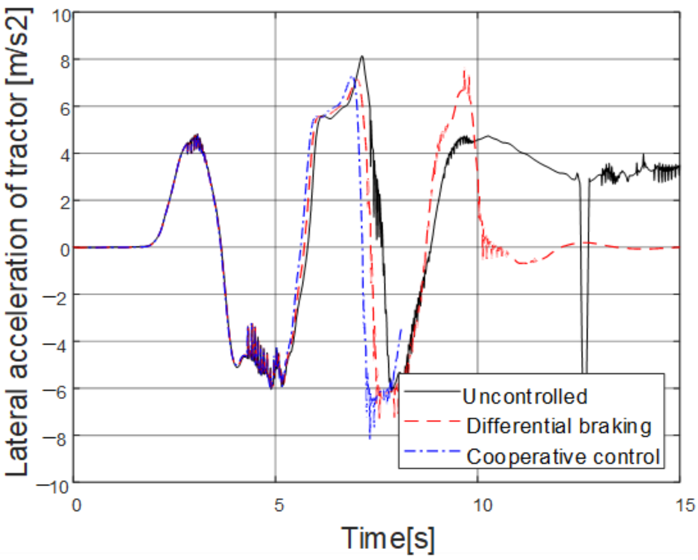

Figure 21. Lateral acceleration of tractor.

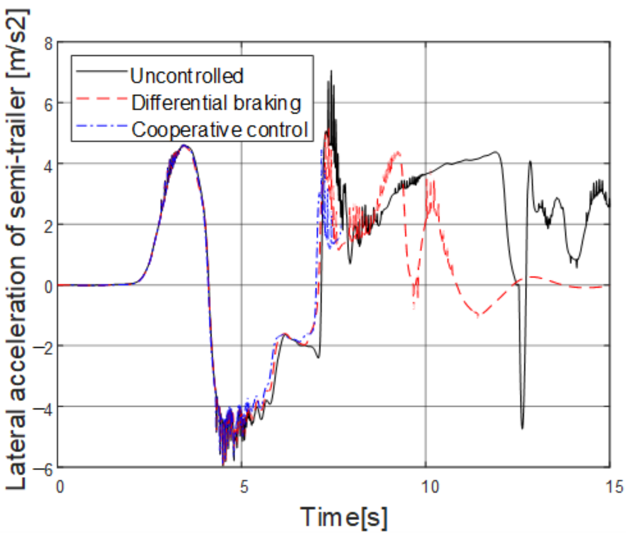

Figure 22. Lateral acceleration of semi-trailer.

In summary, when the control is not added, the tractor semi-trailer has serious sideslip and drift and could even jackknife. The control strategy proposed in the article can effectively restrain the sideslip and jackknife instability, improve the yaw stability and jackknife stability of the tractor semi-trailer, and complete the double-lane-change test. Compared with differential braking control, coordinated control has a faster response speed and faster convergence speed, and it improves the lateral stability of the semitrailer more obviously.

5.2. Step Steering Condition

The initial velocity was defined as v_{x1} = 70 km/h, and the road surface adhesion coefficient was set to 0.3. From the comparison of animation simulation in Figure 23, it can be seen that without control, the tractor semi-trailer experienced sideslip and even jackknife instability and failed to complete the step steering test; after the cooperative and differential controls are added, the tractor semi-trailer has good path tracking ability, which effectively suppresses the occurrence of sideslip and jackknife. The input curve of the steering wheel angle is shown in Figure 24. Figures 25 and 26 show that, without control, the yaw rate of the tractor increases continuously from 7 s to a peak of 46°/s at 14 s. The yaw rate of the semi-trailer increases sharply at 17 s and reaches a peak value of 31.81°/s at 18 s. The tractor semi-trailer has sideslip. After coordinated control and differential braking control are added, the maximum value of the yaw rate of the tractor decreases to 19.34 and 19.93°/s, respectively, and finally tends to 10°/s. The peak value of the yaw rate of the semi-trailer decreases to 17.93 and 17.55°/s, respectively, and finally tends to 10°/s. The response speed of coordinated control is faster than that of differential braking control. Figures 27 and 28 show that, without control, the maximum absolute values of the sideslip angles of the tractor and semi-trailer reach 85.12 and 22.80°, respectively, resulting in serious sideslip. After coordination control and differential braking control are added, the absolute values of the sideslip angles of the tractor are reduced to 13.84 and 17.38°, respectively, and converge to 0 before 15 s. The absolute values of the sideslip angles of the semi-trailer are reduced to 5.95 and 8.12°, respectively, and converge to 0 before 15 s. The response speed and convergence speed of coordinated control are higher than those of differential braking. Figure 29 shows that, without control, the absolute value of the hinge angle reaches 92.53°, and the jackknife phenomenon occurs. After control is added, the absolute value of the maximum value of the hinge angle is reduced to 17° and finally stabilizes at 8°/s. The convergence speed of coordinated control is higher than that of differential braking. Figures 30 and 31 show that, without control, the roll angle of the tractor reaches the peak value of 4.52° at 18 s, the roll angle of the semi-trailer fluctuates greatly, and reaches the peak value of 7.14° at 15.5 s; after the cooperative and differential controls are added, the roll angle of the peak roll angle of the tractor decreases to 2.45 and 2.40°, respectively, and the peak roll angle of the semi-trailer decreases to 3° and 2.95°, respectively. At 15 s, the roll angle of the tractor semi-trailer converges to 2.5 and is finally stable. Figures 32 and 33 show that, without control, the lateral acceleration of the tractor semi-trailer fluctuates greatly and loses control; after adding the cooperative and differential controls, the lateral acceleration of the tractor semi-trailer converges to 3 m/s^2 and is finally stable.

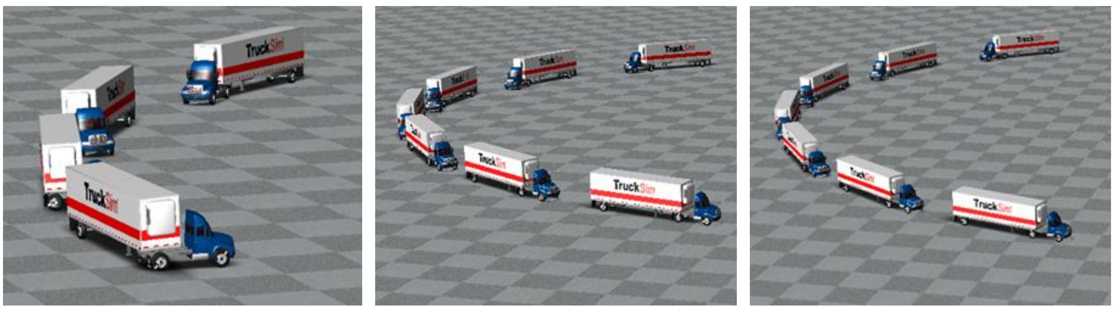

(**a**) With control (**b**) Differential braking control (**c**) coordinated control

Figure 23. Simulation animation comparison.

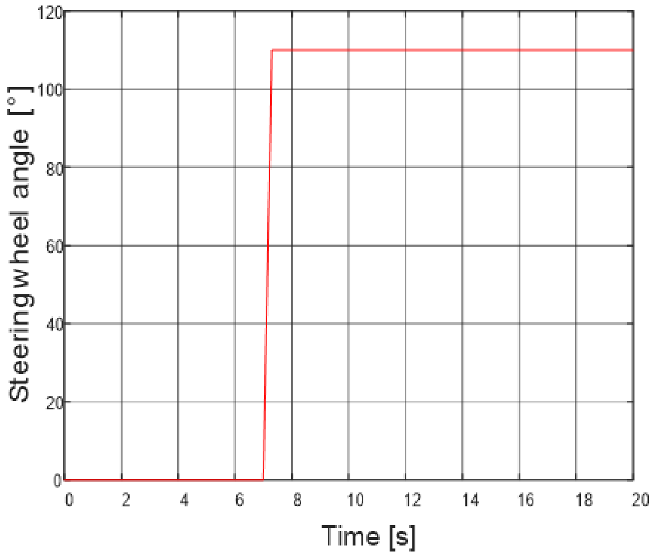

Figure 24. Steering wheel.

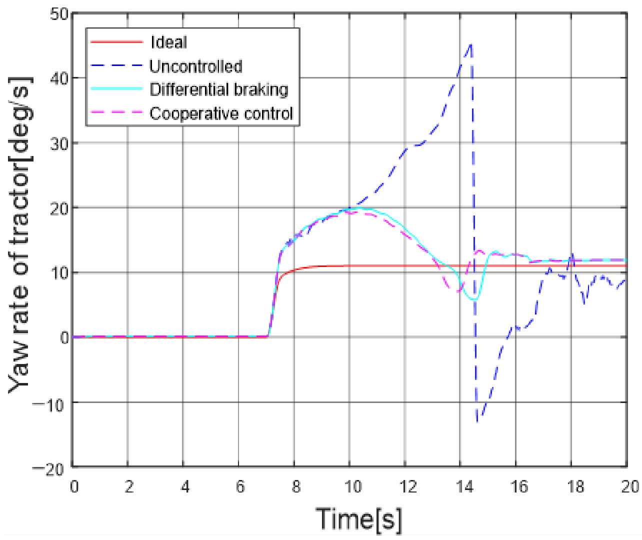

Figure 25. Yaw rate of tractor.

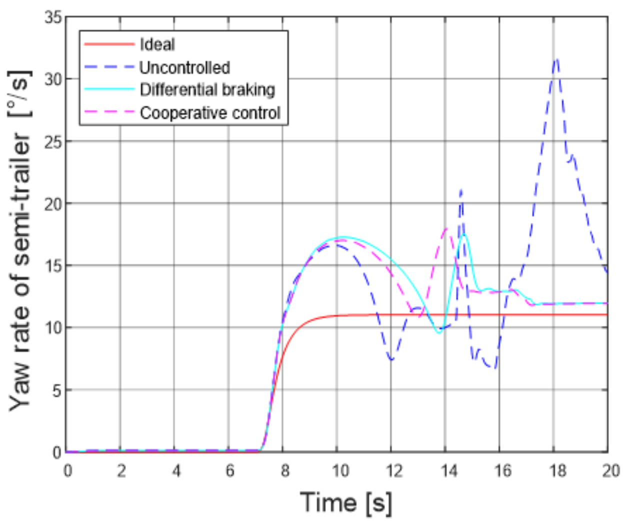

Figure 26. Yaw rate of tractor of semi-trailer.

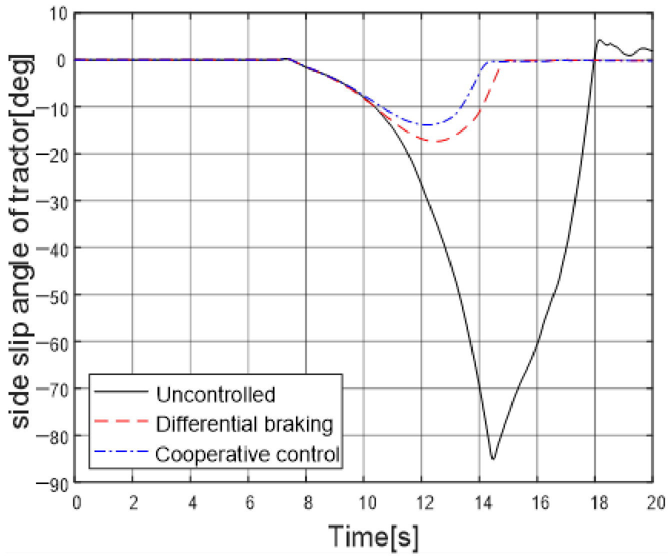

Figure 27. Sideslip angle of tractor.

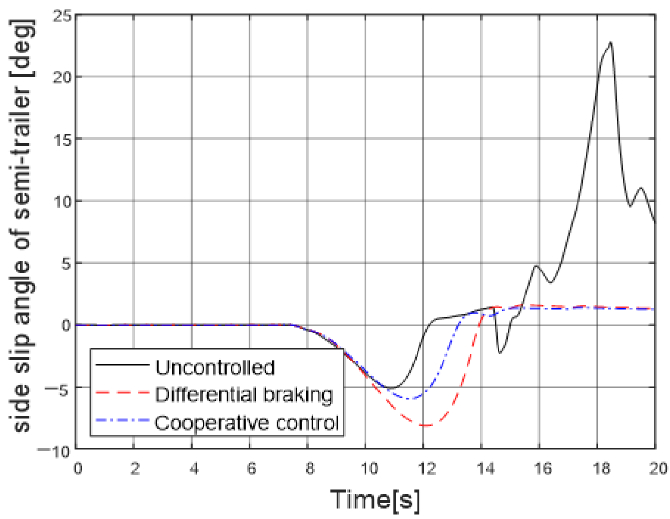

Figure 28. Sideslip angle of semi-trailer.

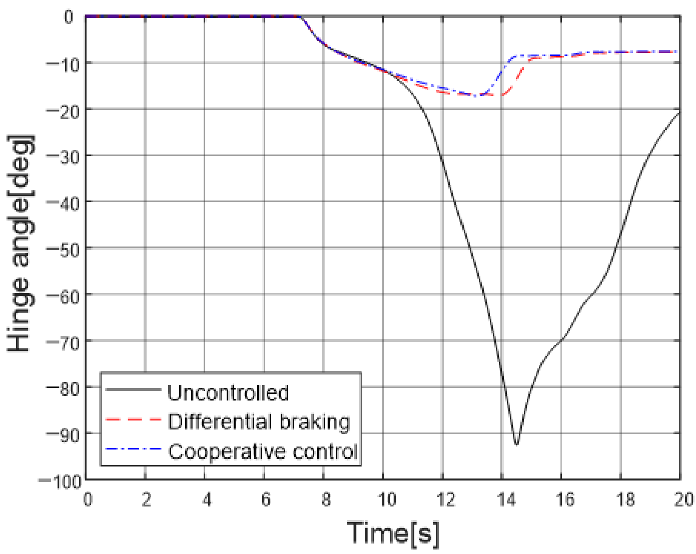

Figure 29. Hinge angle.

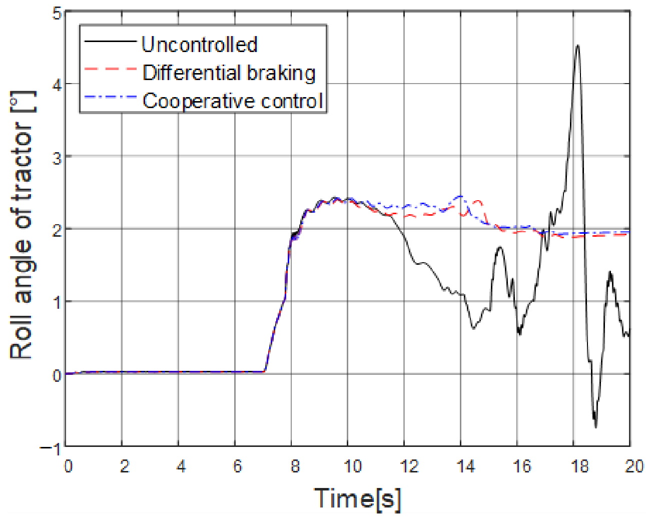

Figure 30. Roll angle of tractor.

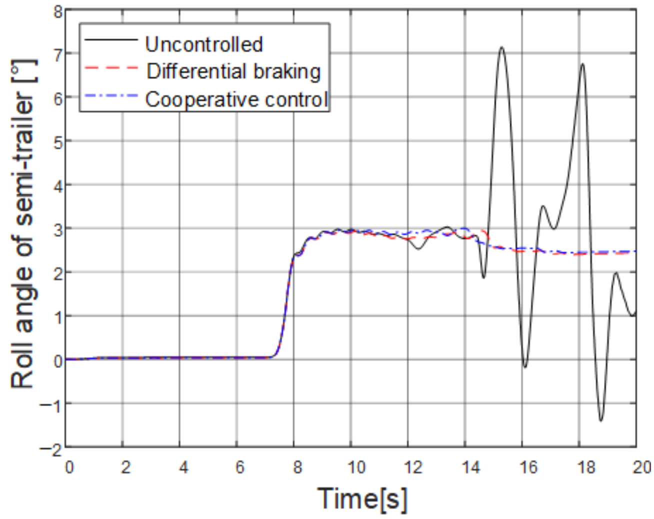

Figure 31. Roll angle of semi-trailer.

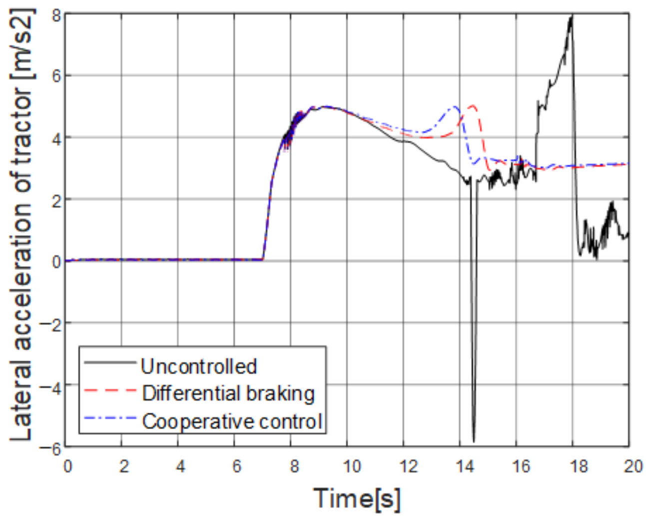

Figure 32. Lateral acceleration of tractor.

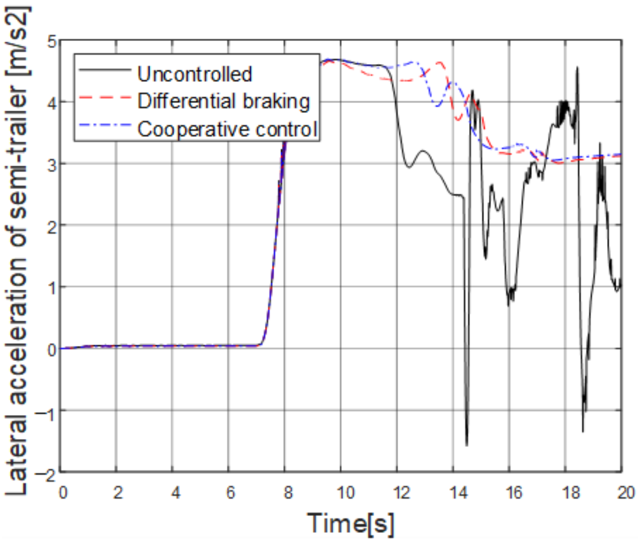

Figure 33. Lateral acceleration of semi-trailer.

In summary, after adding the control, the yaw stability and jackknife stability of the entire vehicle are enhanced, and angle step test is completed. In comparison with differential braking control, the coordinated control strategy has a faster response and faster convergence and can effectively restrain sideslip and jackknife instability and significantly enhance the lateral stability of the tractor semi-trailer.

6. Conclusions

Based on TruckSim and MATLAB/Simulink, a cosimulation model was built, and the yaw rate of the tractor and semi-trailer was considered as the control target. The coordinated control strategy of lateral stability based on coordinated control of a wheel motor electronic differential and mechanical brake was proposed. The simulation verification analysis was carried out under limiting operation condition. The final result shows that the torque distribution rule can realize the desired yaw torque accurately, and the coordinated control strategy of lateral stability exhibits a fast transient response and strong dynamic control ability because of the existence of the hub motor and the coordination with differential braking. Under the condition of a low-adhesion-coefficient road surface, the yaw rate and sideslip angle can track the expected value well and significantly reduce the value of the hinge angle. In comparison with traditional differential braking control (ESP), the coordinated control strategy designed in this article can enhance the lateral stability of a tractor semi-trailer more effectively; the coordinated control strategy has a faster response and faster convergence and can effectively restrain sideslip and jackknife instability and significantly improve the roll stability of the tractor semi-trailer. However, the maximum torque and endurance of the hub motor are a challenge to improve the stability of the tractor semi-trailer. The results show that the combined simulation of TruckSim and Simulink is an effective means for the design and development of the stability control system of the tractor semi-trailer. The cooperative control strategy can better improve the yaw stability; at the same time, it can also improve the roll stability of the vehicle and effectively enhance the running safety of the vehicle.

Author Contributions: Conceptualization, Y.L. (Yufeng Lu) and Z.B.; methodology, Y.L. (Yufeng Lu); software, Z.B.; validation, Y.L. (Yunxia Li); formal analysis, Z.B.; investigation, Y.L. (Yunxia Li); resources, Y.L. (Yufeng Lu); data curation, Z.B.; writing—original draft preparation, Z.B.; writing—review and editing, Y.L. (Yufeng Lu); visualization, Y.L. (Yunxia Li); supervision, Y.L. (Yufeng Lu). All authors have read and agreed to the published version of the manuscript.

Funding: Research on the co construction of enterprises and schools to help local universities develop MOOC (Qilu University of Technology Project 201828).

Conflicts of Interest: The authors declare no conflict of interest.

References

1. Aripin, M.K.; Sam, Y.M.; Danapalasingam, K.A.; Peng, K.; Hamzah, N.; Ismail, M.F. A review of active yaw control system for vehicle handling and stability enhancement. *Int. J. Veh. Technol.* **2014**, *6*, 1–15. [CrossRef]
2. Nie, Z.; Zong, C. Study on parameter identification of simplified model of heavy truck. *Automot. Eng.* **2015**, *6*, 622–630. [CrossRef]
3. Yang, W.; Wei, L.; Liu, J. Joint simulation analysis of lateral stability optimization control of commercial vehicles. *J. Mech. Eng.* **2017**, *2*, 115–123. [CrossRef]
4. Xu, X.; Zhang, L.; Jiang, Y. Active control on path following and lateral stability for truck–trailer combinations. *Arab. J. Sci. Eng.* **2018**, *44*, 1365–1377. [CrossRef]
5. National Highway Traffic Safety Administration. *Traffic Safety Facts 2015*; National Highway Traffic Safety Administration: Washington, DC, USA, 2016.
6. Liu, C.; Guan, Z.; Du, F. Fuzzy PID control of lateral stability of four-wheel steering semitrailer. *Mod. Manuf. Eng.* **2016**, *5*, 47–50.
7. Murata, S. Innovation by in-wheel-motor drive unit. *Veh. Syst. Dyn.* **2012**, *50*, 807–830. [CrossRef]
8. Li, C. An optimal coordinated method for EVs participating in frequency regulation under different power system operation states. *IEEE Access* **2018**, *6*, 62756–62765. [CrossRef]
9. Wang, Q.; Jiang, B.; Li, B.; Yan, Y. A critical review of thermal management models and solutions of lithium-ion batteries for the development of pure electric vehicles. *Renew. Sustain. Energy Rev.* **2016**, *64*, 106–128. [CrossRef]
10. Li, Y.; Li, B.; Xu, X.; Sun, X. A nonlinear decoupling control approachusing RBFNNI-based robust pole placement for a permanent magnet in-wheel motor. *IEEE Access* **2017**, *6*, 1844–1854. [CrossRef]
11. Najjari, B.; Mirzaei, M.; Tahouni, A. Constrained stability control with optimal power management strategy for in-wheel electric vehicles. *Proc. Inst. Mech. Eng. Part K J. Multi-Body Dyn.* **2019**. [CrossRef]
12. Asiabar, A.; Kazemi, R. A direct yaw moment controller for a four in-wheel motor drive electric vehicle using adaptive sliding mode control. *Proc. Inst. Mech. Eng. Part K J. Multi-Body Dyn.* **2019**. [CrossRef]
13. Zhang, Z.; Zhao, W.; Wang, C.; Li, L. Stability control of in-wheel motor electric vehicles under extreme conditions. *Trans. Inst. Meas. Control* **2019**, *41*, 2838–2850. [CrossRef]
14. Tamaddoni, S.; Taheri, S. *Yaw Stability Control of Tractor Semi-Trailers*; SAE Technical Paper 2008-01-2595; SAE: Warrendale, PA, USA, 2008. [CrossRef]
15. Takenaga, H.; Konishi, M.; Imai, J. Route Tracking Control of Tractor-Trailer Vehicles based on Fuzzy Controller. In Proceedings of the Fifth International Workshop on Computational Intelligence & Applications, Hiroshima, Japan, 10–12 November 2009; pp. 105–110.
16. Sogol, K.; Mathias, L.; Jonas, F. Robustness analysis of a steering-based control strategy for improved lateral performance of a truck-dolly-semitrailer. *Int. J. Heavy Veh. Syst.* **2015**, *22*, 1–20.
17. Yang, X.; Kang, N.; Li, X. Stability control of semitrailer train based on TruckSim Simulink joint simulation. *Highw. Transp. Technol.* **2013**, *30*, 141–148.
18. Eunhyek, J.; Kwanwoo, P.; Youngil, K.; Kyongsu, Y.; Kilsoo, K. A tyre slip-based integrated chassis control of front/rear traction distribution and four-wheel independent brake from moderate driving to limit handling. *Veh. Syst. Dyn.* **2018**, *56*, 579–603.
19. Chen, Y.; Chen, S.; Zhao, Y.; Gao, Z.; Li, C. Optimized handling stability control strategy for a four in-wheel motor independent-drive electric vehicle. *IEEE Access* **2019**, *7*, 17017–17032. [CrossRef]
20. Chae, M.; Hyun, Y.; Yi, K.; Nam, K. Dynamic Handling Characteristics Control of an in-Wheel-Motor Driven Electric Vehicle Based on Multiple Sliding Mode Control Approach. *IEEE Access* **2019**, *7*, 132448–132458. [CrossRef]
21. Huang, C.; Lei, F.; Hu, L. Lateral Stability Control Based on Regional Pole Placement of In-wheel-motored Electric Vehicle. *Automot. Eng.* **2019**, *41*, 905–914.
22. Wang, Z.; Wang, Y.; Zhang, L.; Liu, M. Vehicle stability enhancement through hierarchical control for a four-wheel-independently-actuated electric vehicle. *Energies* **2017**, *10*, 947. [CrossRef]
23. Zong, C.; Lin, F.; Hu, L. Control algorithm for braking force distribution of electric control braking system of motor train. In Proceedings of the 2011 Annual Meeting of Society of Automotive Engineering of China, Beijing, China, 26–28 October 2011.

24. Yang, X.; Yang, C.; Zhang, X. Yaw stability control of tractor semi-trailer based on active braking. *Automot. Eng.* **2011**, *33*, 955–961.
25. Gao, H. Research on Braking Direction Stability and Control Strategy of Semitrailer Train. Ph.D. Thesis, Jilin University, Changchun, China, 2014.
26. Zhang, D.; Liu, G.; Zhou, H.; Zhao, W. Adaptive sliding mode fault-tolerant coordination control for four-wheel independently driven electric vehicles. *IEEE Trans. Ind. Electron.* **2018**, *65*, 9090–9100. [CrossRef]
27. Ivanov, V.; Savitski, D. Systematization of integrated motion control of ground vehicles. *IEEE Access* **2015**, *3*, 2080–2099. [CrossRef]
28. Mutoh, N.; Nakano, Y. Dynamics of front-and-rear-wheel-independent-drive-type electric vehicles at the time of failure. *IEEE Trans. Ind. Electron.* **2012**, *20*, 1488–1499. [CrossRef]
29. Chen, Y.; Wang, J. Fast and global optimal energy-efficient control allocation with applications to over-actuated electric ground vehicles. *IEEE Trans. Control. Syst. Technol.* **2012**, *20*, 1202–1211. [CrossRef]
30. Wang, R.; Wang, J. Fault-tolerant control with active fault diagnosis for four-wheel independently driven electric ground vehicles. *IEEE Trans. Veh. Technol.* **2011**, *60*, 4276–4287. [CrossRef]
31. Cheng, Z. Research on the PID control of the ESP system of tractor based on improved AFSA and improved SA. *Comput. Electron. Agric.* **2018**, *148*, 142–147. [CrossRef]
32. Wang, S.; Shi, Y.; Feng, Z. Research on control method based on Fuzzy PID controller. *Mech. Sci. Technol.* **2011**, *30*, 166–172.
33. Jin, X.; Chen, K.; Zhao, Y.; Ji, J.; Jing, P. Simulation of hydraulic transplanting robot control system based on fuzzy PID controller. *Measurement* **2020**, *164*, 108023. [CrossRef]
34. Shi, Q.; Lam, H.; Xuan, C.; Chen, M. Adaptive Neuro-Fuzzy PID Controller based on Twin Delayed Deep Deterministic Policy Gradient Algorithm. *Neurocomputing* **2020**, *402*, 183–194. [CrossRef]
35. Feng, Y.; Wu, M.; Chen, X.; Chen, L.; Du, S. A Fuzzy PID Controller with Nonlinear Compensation Term for Mold Level of Continuous Casting Process. *Inf. Sci.* **2020**, *539*, 487–503. [CrossRef]
36. Liu, Y. Study on Stability of Hydraulic Hybrid Semitrailer Train. Ph.D. Thesis, Qilu University of Technology, Jinan, China, 2019.
37. Guo, K.; Wang, D. Preliminary study on anti slip control theory of automobile drive. *J. Jilin Univ. Technol.* **1997**, *27*, 1–5.